ISPRS Annals of the Photogrammetry, Remote Sensing and Spatial Information Sciences, Volume X-M-1-2023
29th CIPA Symposium "Documenting, Understanding, Preserving Cultural Heritage:
Humanities and Digital Technologies for Shaping the Future", 25–30 June 2023, Florence, Italy

ADAPTION OF INDUSTRIAL NDT PROTOCOLS BASED ON ACTIVE INFRARED THERMOGRAPHY TO THE ART CONSERVATION WORLD: THE CASE OF THE WALL PAINTING AT HERODIUM

Maya Ovadia[1,2] and Anna Brook[2,3]

[1] The Conservation Dept., Israel Antiquities Authority, P.O.B. 586, Jerusalem, Israel - mayao@israntique.org.il
[2] The Spectroscopy and Remote Sensing Laboratory, Dept. of Geography and Environmental Studies, University of Haifa, Israel - abrook@geo.haifa.ac.il
[3] Co-Chair Commission III, WG III/2: Spectral and Thermal Data Processing and Analytics

KEY WORDS: Wall Painting, non-destructive testing (NDT), Infrared Thermography (IRT), Active IRT, Thermographic Signal Reconstruction (TSR).

ABSTRACT:

Salt weathering is one of the most detrimental agents in the deterioration of historic wall paintings. Unfortunately, it is most noticeable once it reaches the surface, and the damage has already been done. Its elusive nature and its integration into the historic structures make it difficult to accurately detect soluble salts at the sub surfaces of wall painting non-destructively. Detailed detection in a delicate artifact such as wall paintings requires custom methodology. The study's case study is the wall painting in Herodium. The wall paintings were severely damaged by salt weathering. Although great efforts were invested in restoring and protecting the paintings their state is still unstable. This study offers a new perspective on the matter utilizing the adaption of industrial protocols based on active Infrared thermography (IRT) with data processing via thermographic signal reconstruction (TSR). The study's primary goal was to optimize the inspection methodology and assist the conservation process with knowledge of soluble salt hazards hidden at the subsurface.

1. INTRODUCTION

Salt crystallization is one of the primary deterioration factors of historic structures, especially of delicate elements such as wall paintings (Abdelaal et al., 2019; Andreas and Zehnder, 1991; Charola and Bläuer, 2015; Doehne, 2002; Martínez-Martínez et al., 2020). An essential step in dealing with salt weathering in wall paintings is an accurate diagnosis of the moisture distribution and the salt content in the wall. Although, obtaining full knowledge of those factors at the subsurface is difficult (Di Tullio et al., 2010). The complexity of the salt deterioration mechanism is due to a couple of intricacies. It's affected by multiple variables: climate and environmental conditions, structure properties, solution properties, kinetic Factors, position, and location (Doehne, 2002; Menéndez, 2018). Moreover, salts are easily transferred as soluble by any amount of water to the structure. Hence, salt crystals as efflorescence or sub-florescence can appear at any location (Arnold and Zehnder, 1989; Charola and Bläuer, 2015). For this reason, fully non-destructive testing (NDT) has been widely preferred for the diagnosis of moisture and salt weathering (Johnston et al., 2019). This study utilized one of the most common and well-established NDT methods, Infrared thermography (IRT) for performing a detailed analysis of salt content at the subsurface of Herudiums' wall paintings.

IRT is widely and extensively applied in the cultural heritage field (Garrido et al., 2021; Mercuri et al., 2015). IRT is utilized according to two different approaches – passive and active. In passive IRT, the inspected radiation source is the target in the object examined, which is usually used for temperature measurement. Active IRT is mainly used for non-destructive testing applications to detect an anomaly in the substance, insulated regions that differ from their surroundings environment (Usamentiaga et al., 2014). In an active IRT analysis, anomalies at the substance are noticeable by a significant temperature shift that could only be obtained by providing a thermal load to the inspected object. The thermal waves created by the stimulator propagate from the surface to the subsurface. When the thermal waves encounter an anomaly, they change their rate. Examining the cooling process after thermal stimulation can help identify the thermal contrast areas causes by anomalies at the subsurface (Castellini et al., 2017; Oswald-Tranta, 2017; Usamentiaga et al., 2014).

However, active thermography has its drawbacks. It is highly dependent on environmental conditions, e.g., the surrounding temperature, airflow and humidity, and non-uniform process caused by uneven heating. Furthermore, IRT measurement suffers from a high signal-noise ratio (SNR), and the thermographic data noise can lose subtle defects or anomalies. These drawbacks make recognizing the of anomalies with delicate nature such as soluble salts difficult (D'Accardi et al., 2019; Usamentiaga et al., 2014). To address the issue, different analysis methods have emerged. Various thermographic image analysis algorithms have been developed for signal enhancement. Algorithms, e.g., principal component thermography (PCT), thermographic signal reconstruction (TSR), and pulsed phase thermography (PPT), are operated under a similar principle. In this principle, the anomaly bodies in the subject are modifying the thermal profile during the cooling period with trends of non-linear behavior (D'Accardi et al., 2019). These algorithms have gained significant popularity in the NDT fields due to the impressive results and discoveries in processing data obtained with active thermography (Balageas et al., 2015; D'Accardi et al., 2019; Fleuret et al., 2020; Oswald-Tranta, 2017). In the art conservation field, pioneer researchers utilize these algorithms based on data obtained with active thermography (Castellini et al., 2017; Mouhoubi et al., 2019).

This study will be focusing on TSR data processing protocols to investigate the time domain in the search for this goal. In TSR, the peaks of the thermal contrast along the first derivative curve

This contribution has been peer-reviewed. The double-blind peer-review was conducted on the basis of the full paper.
https://doi.org/10.5194/isprs-annals-X-M-1-2023-223-2023 | © Author(s) 2023. CC BY 4.0 License.

or second derivative curve indicate anomalies in the subject. In studies from the NDT world, process data via TSR was found to have better sharpness and improved SNR than the raw data (Balageas et al., 2015; Fleuret et al., 2020; Oswald-Tranta, 2017; Zhao et al., 2017). However, these algorithms have not been utilized for the detailed detection of soluble salts at the subsurface of wall paintings.

2. PROTOCOL ADAPTATION DESIGN

2.1 Case Study

Herodium is a palace fortress located south of Jerusalem at the northern edge of the Judaean Desert (Figure 1a). In 2006, the excavations at Mount Herodium, a small royal theater was revealed (Figure 1b). Among the theatre's chambers, one chamber stood out with magnificent secco wall paintings and stucco decorations (Figure 1c). The chamber referred to as the royal box, is considered one of the most impressive decorations ever discovered in Israel (Netzer et al., 2009). Since the exposure, the decorations have decayed and shown severe damage caused by salt crystallization and oxidation (Figure 1d). The conservation project to restore the decoration lasted more than a decay (Neguer and Davidoff, 2015). Though it has been preserved, monitored, and protected by a climate control system, the salts are still present in the walls, and moisture rising has been spotted. The condition of the wall painting is not entirely stable, and they are still in danger.

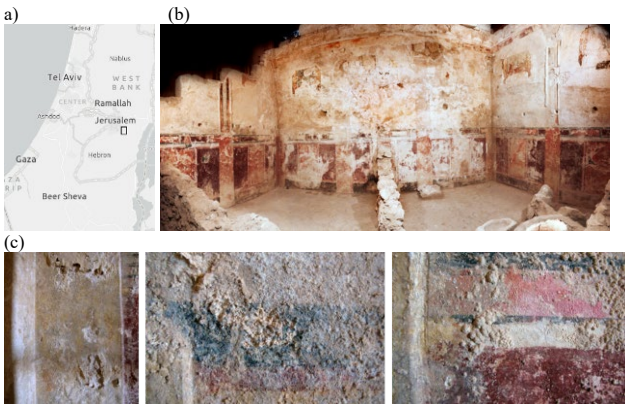

Figure 1. (a) Location map. (b) Panoramic view of the royal box in 2008. (c) Salt effluences in wall paintings in Herodium in 2011 (Neguer and Davidoff, 2015)

2.2 Campaign Setup

The data collecting campaign was designed to collect and record the data obtained via active IRT with continuous heating (Conventional thermography) stimulator transaction. The data-collecting campaign was located at the royal box at Herodium. The framework was set on three of the chamber wall's that are based on the enlargement of the chamber, where the bedrock was carved, plastered, and painted with a single layer of secco wall painting. The framework covered an area of 16 square meters and was divided into 16 sections. The protocol was applied to each section of the framework and the calibration model (Figure 2c), stored on the site. The model was staged on a neutral platform made from wood and kept in a shaded room to keep it dry and away from moisture penetration. The environmental conditions inside the royal room were kept the same since the room is under climate control with an interior temperature of 20° C and a moisture content (MC) of 60%. the protocol consists of three stages. (1) Documentation of the pre-treatment state of the section. With the costume android app. This was conducted for monitoring the process. (2) implementation of an external stimulus. The external stimulus used in this protocol is optical stimulation created with two halogen lamps with a power of 250 watts each. The two lamps were placed one meter from the inspected section's outer surface to achieve a balanced spread of the heat waves (Figures 2a and 2b). The continuous heating was applied for five minutes, causing the wall temperatures to increase by an average of 3 degrees, shifting the mean of the temperature of the sections to approximately 20.5° C. (3) Recording of the cooling period. Immediately after the continuous heating, the recording of the cooling period starts. The recording sequence of the cooling period was set to five minutes long. The data acquisition was conducted using a pre-programmed time-lapse mode in the Therm-App android application. The time-lapse was programmed to a rate of 6 frames a minute, with a ten-second gap between frames, creating a sequence of 30 frames per section at the size of *384*-by-*288* pixels. The campaign was composed of 16 cycles (16 sections) to reach full coverage of the study framework and another cycle on the calibration model.

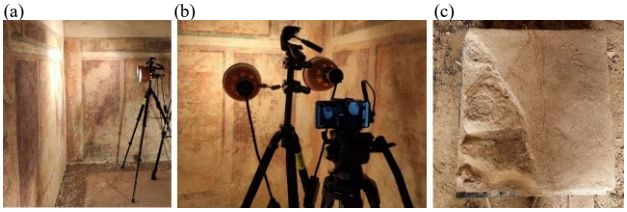

Figure 2. The data collecting instruments. (b) Rear view of the data collecting process inside the royal chamber. (c) the calibration model.

2.3 Data Acquisition

The main instrument used in this study was a Therm-App (Therm-App© by Opgal, Israel), a high-resolution thermal camera for android with an uncooled 17µ Long-Wavelength Infrared (LWIR) detector array, focal lengths of 6.8mm lens (55° x 41°), 13mm lens (29°x 22°), 19mm lens (19°x14°) and 35mm lens (11° x 8°), a spatial resolution of 384 x 288 pixels, measurement accuracy of ±3 ◦C, thermal sensitivity/noise equivalent temperature difference (NETD) is <0.05°C, and spectral range of microbolometer 7.5–14 µm. The Therm-App is a modular device that clips onto an Android device and operates using a custom app called Therm-App by Opgal (THERM-APP™). The thermal-infrared images (PNG format) and data (TXT format) were stored in the memory of an android device. The processing framework was later implemented in MATLAB (MATLAB, R2020b).

2.4 Signal analysis via TSR

In this study, three TSR protocols were utilized for the accurate detection of anomalies for each of the framework sections and the calibration model. Following the protocols, the thermal signal sequence, representing the heat flow over time, was analyzed via the first derivative in the normal time scale and logarithmic scale and with the second derivative in the normal time scale. For comparison, the heat flow was also analyzed via the raw data of the temperatures in the normal time scale. The first TSR protocol used the first der. of temp. in the normal scale as explicit in equation (1). where t denotes the time, and T denotes the temp. After, the pixels values were normalized. The second TSR protocol used the first der. of temp. in the logarithmic scale was conducted as explicit in equation (2). The third TSR proto-

col used the second der. of temp. in the normal scale as explicit in equation (3) (Oswald-Tranta, 2017).

$$x = \frac{d\,(T(t) - T(t=0)}{d\,(t)} \quad (1)$$

$$x = \frac{d(log\,(T(t) - T(t=0))}{d(log\,(t))} \quad (2)$$

$$x = \frac{(d(T(t) - T(t=0))^2}{d\,(t)^2} \quad (3)$$

In addition, in each section, quantitatively analyzed regions of interest (ROIs) were defined allowing follow the heat flow of the thermal load through the inspected subject. The chosen ROIs are belonging to two observed categories - anomalies and natural substance areas. Six ROIs were cropped manually in rectangular window sequences (10-by-10-by-30), according to the heat contrast seen in the data processing of the first derivative in logarithmic scale – three windows focusing on the anomalies and three windows focusing on the natural substance areas. This process was applied to each of the framework sections and the calibration model.

3. RESULTS

The data collected via active IRT displayed the cooling period of the thermal load applied by the stimulus for each pixel in the framework. The raw data and three tested TSR protocols are presented as follows in section 2A of the framework. At first, the heat flow was analyzed through the raw data. The detected anomaly areas stand out in their surroundings by higher temperatures (Figure 3). a thermal gradient cantered in one prominent region that reached a heat contrast of approximately 6º above the min temperature of the surroundings as seen at the beginning of the sequence (0 sec). Though a vignette effect is shown along the cooling process. This effect strongly influences the evaluation of the thermal contrast when the corners of all the sections seem to be much colder than the center of the sections.

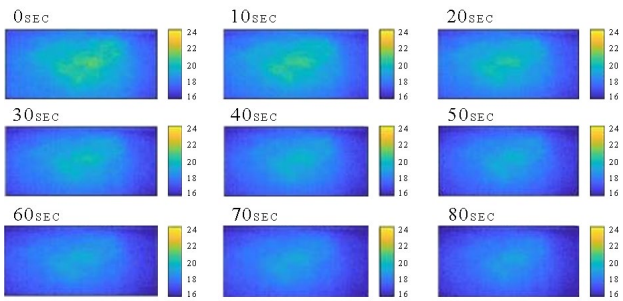

Figure 3. Heat flow based on the raw data in section 2A

To suppress the weakening effects found in the raw data analysis and focus on delicate trends in the heat flow analysis, data processing protocols based on TSR were applied. First, the first der. in a normal scale was examined. The results of this examination (Figure 4) were similar. The output data was noisy and 'flat' with no thermal contrast indicating anomalies. Therefore, this examination was found to be unsuitable for accurate anomaly detection.

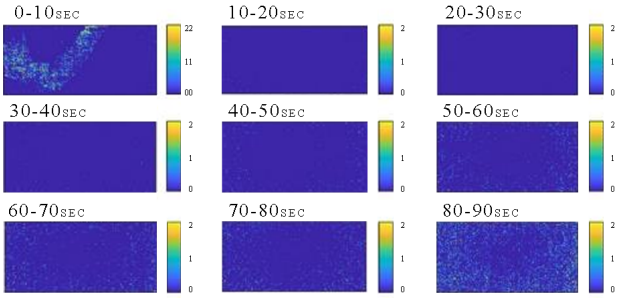

Figure 4. Heat flow based on the first der. on a normal scale in section 2A

Secondly, continuing with the heat flow analysis via data processing protocol based on TSR, the first derivative in the logarithmic scale was utilized to sharpen the data and improve the SNR. The results of the investigation have shown improvement. They are visualizing a gradient of thermal contrast with regional peaks that indicate anomalies. The anomalies detected in section 2A (Figure 5) were observed with a noisy thermal gradient with few local peaks at the beginning of the cooling period. This contrast slowly decayed over time until it disappeared in frame 80-90 sec. In the progressing stages of the cooling period, almost no thermal contrast was observed. However, the heat flow in the calibration model visualized a different phenomenon. In the calibration model, a solid thermal load from the stimulus was observed with no observation of thermal contrast. Importantly, this inspection revealed that the first frame (Figure 5) had been contaminated with the documentation of the stimulator body removal. To eliminate this effect, the first caption of each section sequence was removed.

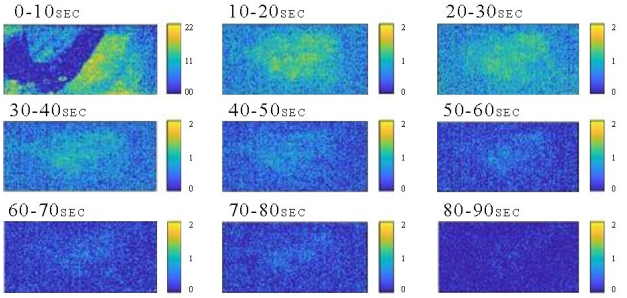

Figure 5. Heat flow based on the first der. in a logarithmic scale in section 2A

To sharpen the results from the invitation with the first derivative in a logarithmic scale, the second derivative in a normal scale was tested. Similar to the first der. in a normal scale inspection, the results (Figure 6) were noisy and 'flat' with no contrast. For these reasons, this examination of the heat flow was found to be unsuitable for accurate anomaly detection.

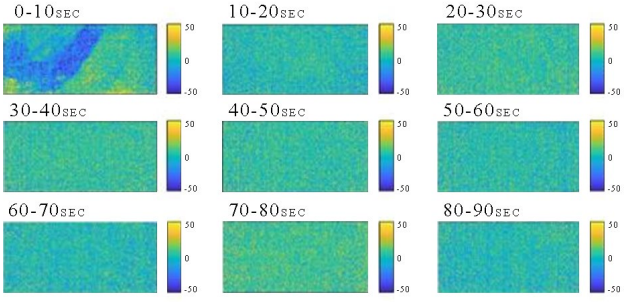

Figure 6. Heat flow based on the second der. on a normal scale in section 2A

Following, an inspection of the thermal contrast in regions of interest (ROIs) was conducted in the row data and the data that was processed with the first der. in logarithmic scale (Figure 7).

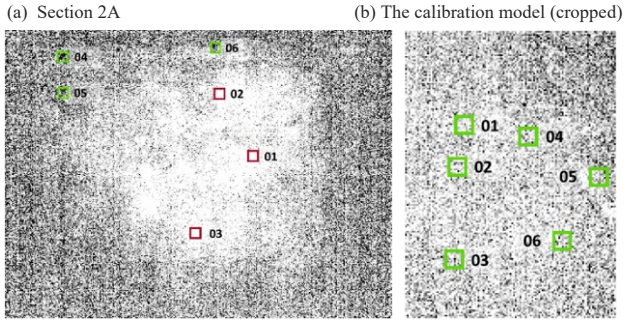

Figure 7. ROIs of the Anomaly (red) and the natural substance (green)

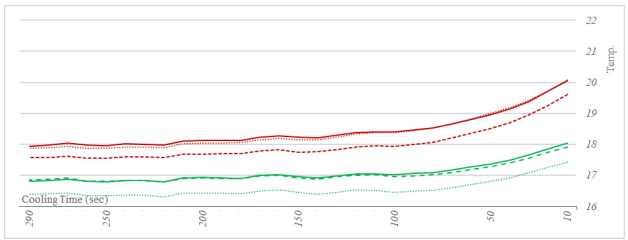

Figure 8. The heat flow in the ROIs, Anomaly (red) and natural substance (green), in section 2A in the raw data

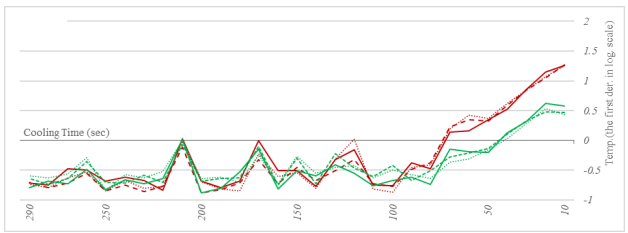

Figure 9. The heat flow in the ROIs, *Anomaly (red) and natural substance (green),* in section 2A in the first der. in log. Scale

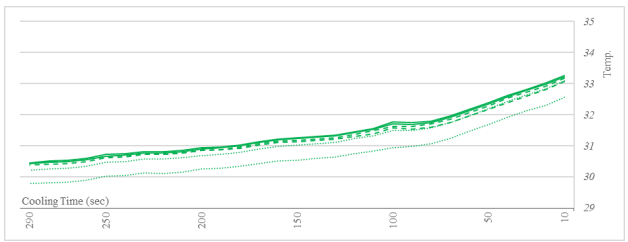

Figure 10. The heat flow in the ROIs, Anomaly (red) and natural substance (green), in the calibration model in the raw data

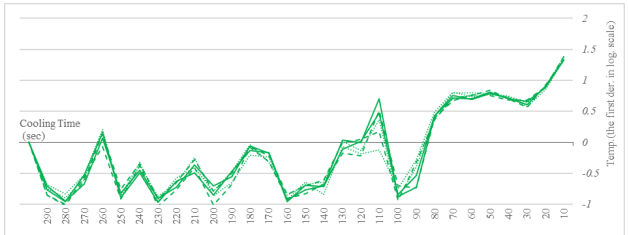

Figure 11. The heat flow in the ROIs, Anomaly (red) and natural substance (green), in the calibration model in the first der. in log. scale

Figure 8 describes the thermal contrast between the two ROIs categories with the processed data with the first derivative in a logarithmic scale. There is a noticeable difference in the heat flow curves of the two ROIs groups in the first 90 sec of the cooling period. ROIs 01-03 represent the detected anomaly with a much higher score than ROIs 04-06 representing the natural substance. The thermal contrast between the two groups decayed with the passing time until 90 sec where no obvious contrast is shown. Another interesting inspection is the high similarity between the two groups themself in their thermal behavior throughout the cooling period. In figure 9 the anomaly group, represented with ROIs 01-03, reached much higher temperatures in compression with the natural substance group, represented with ROIs 04-06, throughout the cooling process. This observation contrasts the ROIs thermal contrast analysis of the first derivative in logarithmic scale (figure 8) that showed a clear trend of decay in thermal contrast until it disappears in 50-90 sec of the cooling period. Another observation is the smoothness of the heat flow curves in all the chosen sections. Adding to the previous observation, this phenomenon is turning the raw data analysis less informative. Figure 10 and Figure 11 describe the ROIs in the calibration model. The heat flow curves of all six ROIs are almost identical throughout the entire cooling period in the raw data (Figure 10) and in the processed data (Figure 11). These observations are added to the previous statements and strengthen the calibration model has proven to be a 'clean' control group with no soluble salts within.

4. DISCUSSION AND CONCLUSIONS

IRT is widely used in the art conservation field for the structure analysis and detection of deterioration faults at the surface and subsurface, e.g., moisture and sub-superficial defects as micro-cracks and detachments (Bison et al., 2014; Sfarra et al., 2012, 2018). Although, the common day-to-day use of thermal inspection is a conventional use with a passive IRT. This method does not reveal all problems immediately and accurately. With no thermal stimulation was made in which the salts start to react. This study adapted industrial protocols based on active IRT with data TSR. the results indicate that Active IRT with STR data processing protocols were successful for fully non-destructive accurate detection of soluble salts in the large body of the subsurface of a wall painting at the pixel level. This knowledge of the subsurface can help the conservation process before the appearance of weathering signs.

Although, the data collection process via the active IRT faced some challenges. the IRT camera created a vignette effect that made non-homogeneous surface heating. The second challenge appeared in the measurement process where the stimulator left 'burn' marks in the data. These marks in the shape of a massive thermal load were screening the informative data. These disadvantages strengthen the purpose of data processing techniques in analysing thermal data collected via active IRT. These techniques are extensively used in many industries and were proven to be effective in anomaly detection by enhancing and sharpening the input signal and allowing deeper defect detection. This study focused on Thermographic Signal Reconstruction (TSR). The TSR can be well implemented in the time domain at a normal scale, as was presented by Zhao et al. (Zhao et al., 2017). The use of data processing presented an enhancement and sharpening of the input signal. Although not all TSR protocols showed successful results and can be taken for the test. Subtle details in the detected anomalies were successfully observed in the heat flow sequence of the cooling period via the first dev. in log. scale. The study's base assumption was that the anomaly's

This contribution has been peer-reviewed. The double-blind peer-review was conducted on the basis of the full paper.
https://doi.org/10.5194/isprs-annals-X-M-1-2023-223-2023 | © Author(s) 2023. CC BY 4.0 License.

source was the soluble salts present at the subsurface. This assumption was tested positive with aid of a calibration model proven to be homogenous with no anomaly.

This study has taken data processing methods from the industrial NDT fields and adapted them to the art conservation world. Though, it was not possible to take the same protocols and apply them unchanged to monuments such as wall paintings. Since the subject is extremely vulnerable and valuable, it cannot be treated as an industrial element that can stand an instance of thermal load. Moreover, unlike the industrial fields where the defect is fairly different from the inspected element. In the case of soluble salts are well integrated with diffusion with the moisture into the wall. Therefore, the work must be sensitive and delicate, and it cannot be treated as an industrial element that can stand a massive thermal load. This fact causes the use of a much-reduced impact of the stimulator on the inspected wall painting. To compensate for that utilizing the first derivative on a logarithmic scale on thermal data was used. The results support the existing theories of the ability of data processing techniques to enhance and sharpen the input signal and overcome a reduced thermal impact.

This data processing is only the first step in a spectral vision. The timeline can be taken as a series of wavelets and the signature of the heat flow can be assess like a spectral signature for detailed detection of the anomalies at the pixel level. Eventually, the anomalies can be translated to soluble salts with a well-known index, A Salinity index (SI). These proposed spectral methods, a well-known index with the presented adaptation of NDT protocol can assist in the early identification of evolving hazards and prevention of unnecessary damage. While those methods combined are not common in the art conservation field to detect soluble salts, they can significantly benefit it.

ACKNOWLEDGMENTS

This study was conducted with the help of OPGAL. The company has supplied the Therm-App, a Thermal camera, that was used for collecting data. The study is also conducted with the help and guidance of the art conservation department at the Israel Antiquities Authority (IAA), Responsible for the conservation project of the decoration at Herodium. The department has created the calibration model and the laboratory samples while the head of the department will take part in the validation stage of the study. We would like to extend my sincere thanks to Mr. Jacques Neguer, The Formal head of the art conservation department at the Israel Antiquities Authority, for his support and guidance in this proposed study design.

REFERENCES

Abdelaal, S., Yamani, R., Abdel-fatah, M., & Sandu, I. G. (2019). Conservation Science Salt Weathering of Imni Tomb . *International Journal of Conservation Science*, *10*(4), 661–680.

Arnold, A., and Zehnder, K. (1989). Salt weathering on monuments. *La Conservazione Dei Monumenti Nel Bacino Del Mediterraneo*.

Arnold, A., and Zehnder, K. (1991). Monitoring wall paintings affected by soluble salts. *The Conservation of Wall Paintings: Proceedings of a Symposium Organized by the Courtauld Institute of Art and the Getty Conservation Institute, London, July 13–16, 1987*, *September*, 103–35. http://192.215.101.9/conservation/publications_resources/pdf_publications/wall_paintings.pdf#page=130

Balageas, D. L., Roche, J.-M., Leroy, F.-H., Liu, W.-M., and Gorbach, A. M. (2015). *THE THERMOGRAPHIC SIGNAL RECONSTRUCTION METHOD: A POWERFUL TOOL FOR THE ENHANCEMENT OF TRANSIENT THERMOGRAPHIC IMAGES*. National Institutes of Health. https://www.ncbi.nlm.nih.gov/pmc/articles/PMC4321698/

Bison, P., Bortolin, A., Cadelano, G., Ferrarini, G., Lopez, F., and Maldague, X. (2014). *Evaluation of frescoes detachments by partial least square thermography*. https://doi.org/10.21611/qirt.2014.109

Castellini, P., Martarelli, M., Lenci, S., Quagliarini, E., Silani, M., and Martellone, A. (2017). Diagnostic survey on frescoes paintings in Pompei by active Ir-thermography. *IMEKO International Conference on Metrology for Archaeology and Cultural Heritage, MetroArchaeo 2017*, 51–56.

Charola, A. E., and Bläuer, C. (2015). Salts in Masonry: An Overview of the Problem. *Restoration of Buildings and Monuments*, *21*(4–6), 119–135. https://doi.org/10.1515/rbm-2015-1005

D'Accardi, E., Palano, F., Tamborrino, R., Palumbo, D., Tatì, A., Terzi, R., and Galietti, U. (2019). Pulsed Phase Thermography Approach for the Characterization of Delaminations in CFRP and Comparison to Phased Array Ultrasonic Testing. *Journal of Nondestructive Evaluation*, *38*(1), 1–12. https://doi.org/10.1007/s10921-019-0559-8

Di Tullio, V., Proietti, N., Gobbino, M., Capitani, D., Olmi, R., Priori, S., Riminesi, C., and Giani, E. (2010). Non-destructive mapping of dampness and salts in degraded wall paintings in hypogeous buildings: The case of St. Clement at mass fresco in St. Clement Basilica, Rome. *Analytical and Bioanalytical Chemistry*, *396*(5), 1885–1896. https://doi.org/10.1007/s00216-009-3400-x

Doehne, E. (2002). Salt weathering: A selective review. *Geological Society Special Publication*, *205*(January 2002), 51–64. https://doi.org/10.1144/GSL.SP.2002.205.01.05

Fleuret, J., Ebrahimi, S., and Maldague, X. (2020). Pulsed Thermography Signal Reconstruction Using Linear Support Vector Regression. *The 15th Quantitative InfraRed Thermography (QIRT) Conference*. https://doi.org/10.21611/qirt.2020.150

Garrido, I., Erazo-Aux, J., Lagüela, S., Sfarra, S., Ibarra-Castanedo, C., Pivarčiová, E., Gargiulo, G., Maldague, X., and Arias, P. (2021). Introduction of deep learning in thermographic monitoring of cultural heritage and improvement by automatic thermogram pre-processing algorithms. *Sensors (Switzerland)*,

21(3), 1–44. https://doi.org/10.3390/s21030750

Johnston, B. J., Ruffell, A., Warke, P., and McKinley, J. (2019). 3DGPR for the Non-Destructive Monitoring of Subsurface Weathering of Sandstone Masonry. *Heritage*, *2*(4), 2802–2813. https://doi.org/10.3390/heritage2040173

Martínez-Martínez, J., Torrero, E., Sanz, D., and Navarro, V. (2020). Salt crystallization dynamics in indoor environments: Stone weathering in the Muñoz Chapel of the Cathedral of Santa María (Cuenca, central Spain). *Journal of Cultural Heritage*.
https://doi.org/10.1016/j.culher.2020.09.011

MATLAB, The MathWorks Inc. (2020). Optimization Toolbox version: 9.0 (R2020b), Natick, Massachusetts: The MathWorks Inc. https://www.mathworks.com

Menéndez, B. (2018). Estimators of the impact of climate change in salt weathering of cultural heritage. *Geosciences (Switzerland)*, *8*(11). https://doi.org/10.3390/geosciences8110401

Mercuri, F., Cicero, C., Orazi, N., Paoloni, S., Marinelli, M., and Zammit, U. (2015). Infrared Thermography Applied to the Study of Cultural Heritage. *International Journal of Thermophysics*, *36*(5–6), 1189–1194. https://doi.org/10.1007/s10765-014-1645-x

Mouhoubi, K., Detalle, V., Vallet, J. M., and Bodnar, J. L. (2019). Improvement of the non-destructive testing of heritage mural paintings using stimulated infrared thermography and frequency image processing. *Journal of Imaging*, *5*(9). https://doi.org/10.3390/jimaging5090072

Neguer, J., and Davidoff, N. (2015). *Herodium, The Royal chamber, Conservation Project - Wall paintings and decoration*.

Netzer, E., Porat, R., Kalman, Y., and Chachy-Laureys, R. (2009). Herod’s Grave and the Royal Theater on the slope of the Herodium Hill. *Qadmoniyot*, *138*, 104–117.

OPGAl. (2019). Therm-App™ [Mobile app]. App store. https://play.google.com/store/apps/details?id=com.thermapp&hl=he&gl=US

Oswald-Tranta, B. (2017). Time and frequency behaviour in TSR and PPT evaluation for flash thermography. *Quantitative InfraRed Thermography Journal*, *14*(2), 164–184. https://doi.org/10.1080/17686733.2017.1283743

Sfarra, S., Fernandes, H. C., López, F., Ibarra-Castanedo, C., Zhang, H., and Maldague, X. (2018). Qualitative Assessments via Infrared Vision of Sub-surface Defects Present Beneath Decorative Surface Coatings. *International Journal of Thermophysics*, *39*(1), 1–24. https://doi.org/10.1007/s10765-017-2333-4

Sfarra, S., Ibarra-Castanedo, C., Ambrosini, D., Paoletti, D., Bendada, A., and Maldague, X. (2012). Non-Destructive Testing Techniques to Help the Restoration of Frescoes. *Arabian Journal for Science and Engineering*, *39*(5), 3461–3480. https://doi.org/10.1007/s13369-014-0992-z

Usamentiaga, R., Venegas, P., Guerediaga, J., Vega, L., Molleda, J., and Bulnes, F. G. (2014). Infrared thermography for temperature measurement and non-destructive testing. *Sensors (Switzerland)*, *14*(7), 12305–12348. https://doi.org/10.3390/s140712305

Zhao, Y., Mehnen, J., Sirikham, A., and Roy, R. (2017). A novel defect depth measurement method based on Nonlinear System Identification for pulsed thermographic inspection. *Mechanical Systems and Signal Processing*, *85*, 382–395. https://doi.org/10.1016/j.ymssp.2016.08.033